Determination of Transmittance of IR Windows made of CaF_2 within Operational Temperatures of Electric Devices

Krzysztof Dziarski
Poznań University of Technology, Institute of Electric Power Engineering, Piotrowo 3A, 60-965 Poznań, Poland

Arkadiusz Hulewicz
Poznań University of Technology, Institute of Electrical Engineering and Industry Electronics, Piotrowo 3A, 60-965 Poznań, Poland

Abstract: The article presents summaries of works which have resulted in the presentation of a formula making it possible to determine an approximate transmittance of an IR window used in thermographic measurements of electric device temperatures. The equation was formulated after analysing components of the IR radiation reaching the camera lens in case when an IR window was not used and when an IR window was used. Conditions prevailing in course of the thermographic temperature measurement of electric devices contained in the switchgear were recreated in the performance of the works. The measurement system which was used in the experiment has been presented. Components of the IR radiation reaching the camera lens in case when the IR window was used and when the IR window was not used have been discussed. The obtained transmittance results of windows VPFR-75 FRK100-CL have been compared against data from literary sources.

Słowa kluczowe: thermography, electric devices, metrology

1. Introduction

Diagnostics of electrical devices, understood as cyclical monitoring, the assessment of proper operation and in the case of detection of irregularities, identification of the source of the problem, plays an important role [1].

An excessive increase of temperature of electric devices may lead to a serious failure. An excessive temperature of current circuits can cause their structure to change and, consequently, can cause their shape to irreversibly change and a short-circuit to occur [2, 3].

In case of current rails, temperature over the softening point also causes the inner structure of the current rail to irreversibly change and the current rail to yield.

The temperature of the wire used to connect the electric devices is also important. An excessive temperature of an operational conductor may cause insulation to become damaged and, consequently, it may lead to short-circuits between individual conductors of wires in a bundle [4].

Autor korespondujący:
Krzysztof Dziarski, krzysztof.dziarski@put.poznan.pl

Artykuł recenzowany
nadesłany 06.08.2021 r., przyjęty do druku 21.10.2021 r.

Heating of operational conductors of wires, current rails and current circuits of switchgears is related to the flow of operational current or, in case of interferences, a short-circuit current. Information about the temperature of these devices makes it possible to answer a question how much one can load a given element while still being able to ensure failure-free operation.

Electric devices are often installed in switchgears. It may be hazardous or, in some cases, impossible to measure the temperature of an electric device, wire or current rail by means of a temperature contact sensor [6].

It is possible to employ the thermographic temperature measurement to improve the safety of the person performing the measurement. An additional advantage of this contactless method is the registration of distribution of temperatures over the selected area.

Registration of an improper distribution of temperatures on the surface of elements will allow one to detect failure before it occurs. In consequence, it is possible to plan the repair in such a way as to reduce the device downtime-related costs.

Despite essential advantages, thermography also has drawbacks. It is an imprecise method. Additionally, the measurement result depends on a number of factors. The most important factors determining the value of the thermographic temperature measurement include: emissivity coefficient value [7], reflected temperature [8], distance between the thermographic camera lens and the surface under observation [9], ambient temperature [10], temperature of the external optical system [11], transmission of the external optical system [12], air humidity [13] and registered thermogram sharpness [14].

In practice, an IR window is often installed in switchgear doors. When the IR window is used, it is no longer necessary to open the switchgear during the measurement. Furthermore, the use of an IR window increases the safety of the person performing the measurement [15].

Two kinds of IR windows are used: crystalline and polymer-reinforced. IR windows can also be broken down by the length of the IR radiation waves.

In case of the infrared radiation within the LWIR (Long Wavelength Infrared) range, the frequently used material is calcium fluoride, CaF_2, while in case of the radiation within the MWIR (Medium Wavelength Infrared) range, magnesium oxide MgF_2 is often used to manufacture windows [17, 18].

However, no IR window lets through 100 % of the IR infrared radiation. This means that some IR radiation reaching the camera lens is suppressed by the window.

The issue of limited transmission of the IR radiation through the IR window is particularly important in the quantitative thermography when it is important to precisely measure the temperature of the surface under observation. When an IR window is placed between the object under observation and the thermographic camera lens, the radiation beam reaching the camera lens will be weaker. Consequently, the thermographic camera indication will be underrated.

Therefore the information enabling compensation of the external optical window effect is important. Literary sources describe the dependency transmittance of the CaF_2 and MgO windows on the transmitted radiation wavelength. The authors, however, have not found a description of a method enabling one to independently determine the IR window transmittance. Therefore, research works were undertaken in order to demonstrate the way to determine the transmittance of a crystalline IR window made of CaF_2. To validate the method presented, it was decided to determine the transmittance values for the IR windows made of CaF_2 and to compare the values obtained against the data from the literary sources.

2. Methodology

2.1. Measurement System

The undertaken research works required a measurement system to be designed. Its major part was an infrared radiator. The radiator employed consisted of two parts – an aluminium block sized 21 cm × 21 cm coated with the Velvet Coating 811-21 paint and a radiator temperature control system [19].

The radiator has been designed in such a way as to emit IR radiation only in one direction. The emissivity coefficient ε of the paint which was used to paint the radiator has been determined within a range from –36 °C to 82 °C. The uncertainty with which the emissivity coefficient was determined was 0.004 [19]. The radiator surface temperature was measured by means of a thermocouple with a 0.1 °C resolution.

While taking the measurements, the radiator temperature was changed within a range from 37.7 °C to 70 °C. The lower limit of the range is the design temperature (according to PN-HD 60364-5-52), arbitrarily increased so as to keep the radiator temperature significantly higher than the ambient temperature. The upper limit of the assumed temperature range is the acceptable temperature of the wire conductor in a polyvinyl chloride (PVC) insulation [20].

The acceptable temperature of the wire conductor in a polyvinyl chloride (PVC) insulation is lower than the copper softening point (190–200 °C) [21] and the aluminium softening point (100–150 °C). It was decided to select the lowest of the aforementioned acceptable temperatures as the upper limit of the adopted range.

The radiator was placed inside a metal box sized 50 cm × 50 cm × 50 cm. A 7.5 cm diameter hole was bored in the face wall of the box. Crystalline IR windows VPFR-75 (IRISS, Bradenton, Florida, USA) [22] and FRK100-CL (Fluke, Evererett, Washington, USA) [23] were alternately placed in the hole. The IR windows used are presented (Fig. 1).

The Flir E50 thermographic camera (Flir, Winsonville, Oregon USA) [24] was brought to the IR window (Fig. 2).

a) b)

Fig. 1. IR windows being used: a) VPFR-75, b) FRK100-CL
Rys. 1. Wykorzystane okna transmisyjne: a) VPFR-75, b) FRK100-CL

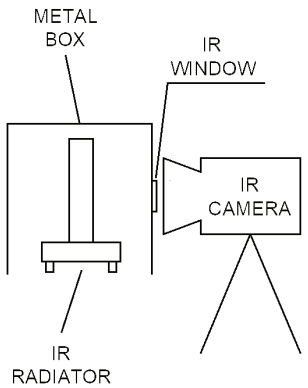

Fig. 2. Designed measurement station
Rys. 2. Skonstruowane stanowisko pomiarowe

2.2. IR Window Transmittance

The IR window transmittance is a ration of the IR radiation registered in two cases – when the IR radiation reaches the thermographic camera lens through the IR window and when the IR radiation reaches the thermographic camera lens directly. The IR window transmittance can be described by means of formula (1).

$$\tau_w = \frac{W_w}{W_d} = \frac{\sigma \cdot \vartheta_1^4}{\sigma \cdot \vartheta_2^4}, \quad \vartheta_2 > \vartheta_1 \tag{1}$$

where: τ_w – IR window transmittance, W_w – IR radiation reaching the camera lens through an IR window, W_d – IR radiation reaching the thermographic camera lens directly, ϑ_1 – temperature indicated by the thermographic camera after an IR window has been used, ϑ_2 – temperature indicated by the thermographic camera without an IR window being used, σ – the Boltzmann constant equal to 5.67 cm × 10^{-8} W/(m^2 · K^4).

One should notice that formula (1) is correct in case of a black body. While analysing a real case, one should take into account the following factors. For this purpose, the component values W_w and W_d should be analysed.

When the IR radiation directly reaches the thermographic camera lens, it consists of three components: radiation emitted by the radiator (2), radiation reflected from the radiator (3) and

radiation emitted by air particles situated between the radiator and the thermographic camera lens (4) [25].

$$\varepsilon_r \cdot W_{obj} \cdot \tau_a \tag{2}$$

$$(1-\varepsilon_r) \cdot W_{reflr} \cdot \tau_a \tag{3}$$

$$(1-\tau_a) \cdot W_a \tag{4}$$

where: W_{obj} – radiation emitted by the radiator, ε_r – emissivity coefficient, τ_a – atmosphere transmittance coefficient, W_{reflr} – radiation reflected from the infrared radiator, W_a – radiation emitted by air particles situated between the infrared radiator and thermographic camera lens.

After taking the Stefan-Boltzmann law into account and summing up equations (2–4), value W_d can be described by means of equation (5)

$$W_d = \varepsilon_r \cdot \sigma \cdot \vartheta_{obj}^4 \cdot \tau_a + (1-\varepsilon_r)\sigma \cdot \vartheta_{reflr}^4 \cdot \tau_a + (1-\tau_a)\sigma \cdot \vartheta_a^4 \cdot \tau_a \tag{5}$$

where: ϑ_{obj} – radiator surface temperature, ϑ_{reflr} – temperature reflected from the radiator surface, ϑ_a – ambient temperature.

Components of the IR radiation reaching the IR camera lens are shown (Fig. 3). This components has been also showed in [26, 27].

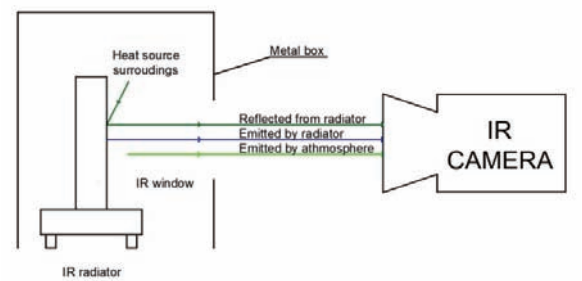

Fig. 3. Components of the IR radiation reaching the thermographic camera lens in case when no IR window is used
Rys. 3. Składowe promieniowania IR docierającego do obiektywu kamery termowizyjnej w przypadku, gdy nie zastosowano okna transmisyjnego

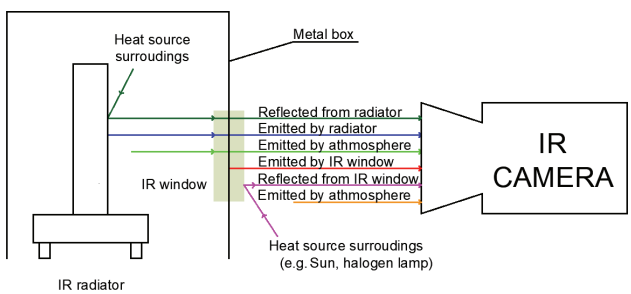

Fig. 4. Components of the IR radiation reaching the thermographic camera lens in case when an IR window is used
Rys. 4. Składowe promieniowania IR docierającego do obiektywu kamery termowizyjnej w przypadku, gdy zastosowano okno transmisyjne

After using an IR window, the analysis of components of the radiation reaching the camera lens W_w is more difficult [15]. Apart from the components described in equations (2)–(4), additional factors should be taken into account. In the case being analysed, equation (2) takes the form of equation (6) and equation (3) takes the form of equation (7). In addition, one should also take into account the IR radiation emitted by the IR window surface (8) and the IR radiation reflected from the IR window surface (9). In the case being discussed, one can distinguish between two air layers situated between the IR radiator and the IR window as well as between the IR window and the IR radiator. Therefore one should take into account both the radiation emitted by the air layer situated between the radiator and the IR window (10) as well as the radiation between the IR window and the thermographic camera lens (11).

The distribution of the IR radiation reaching the thermographic camera lens in the case of using the IR window has been showed in [27, 28] and presented in this article (Fig. 4).

$$\varepsilon_r \cdot W_{obj} \cdot \tau_{a1} \cdot \tau_{a2} \cdot \tau_w \tag{6}$$

$$(1-\varepsilon_r) \cdot W_{reflr} \cdot \tau_{a1} \cdot \tau_{a2} \cdot \tau_w \tag{7}$$

$$(1-\tau_w) \cdot W_w \tag{8}$$

$$(1-\varepsilon_w) \cdot W_{reflw} \tag{9}$$

$$(1-\tau_{a1}) \cdot W_{amb1} \cdot \tau_{a2} \cdot \tau_w \tag{10}$$

$$(1-\tau_{a2}) \cdot W_{amb2} \tag{11}$$

where: W_{reflr} – radiation reflected from the radiator, τ_1 – transmittance of the air layer between the radiator and the box, τ_2 – transmittance of the air layer between the box and the thermographic camera lens, W_{amb1} – radiation of the air layer between the radiator and the box, W_w – radiation emitted by the IR window, τ_w – IR window transmittance, W_{amb2} – radiation of the air layer between the box and the thermographic camera lens, ε_w – emissivity coefficient of the IR window, W_{reflw} – radiation reflected from the IR window.

In order to reduce the number of variables in the final equation, the following simplifications (12)–(14) have been adopted:

$$\tau_{a1} = \tau_{a2} = \tau_a \tag{12}$$

$$W_{amb1} = W_{amb2} = W_a \tag{13}$$

$$\vartheta_w = \vartheta_a \tag{14}$$

where: ϑ_w – IR window temperature, ϑ_a – air temperature.

Value W_w being a sum of equations (6)-(11) is presented in equation (15). The Stefan-Boltzmann law and equations (12)–(14) are taken into account.

$$\begin{aligned} W_w = {} & (1-\varepsilon_r)\sigma \cdot \vartheta_{reflr}^4 \cdot \tau_a^2 \cdot \tau_w + \varepsilon_r \cdot \sigma \cdot \vartheta_{obj}^4 \cdot \tau_a^2 \cdot \tau_w + \\ & + (1-\tau_a)\sigma \cdot \vartheta_a^4 \cdot \tau_a \cdot \tau_w + (1-\tau_w)\sigma \cdot \vartheta_a^4 \cdot \tau_a + \\ & + (1-\tau_a)\sigma \cdot \vartheta_a^4 + (1-\varepsilon_w)\sigma \cdot \vartheta_{reflw}^4 \end{aligned} \tag{15}$$

By inserting equation (5) and (15) into equation (1) and making transformations, one can obtain equation (16) which makes it possible to determine the transmittance of the IR window being used.

$$\tau_w = \frac{\frac{A}{W_d} - \left[(1-\tau_a)\sigma \cdot \vartheta_a^4 + (1-\varepsilon_w)\sigma \cdot \vartheta_{reflr}^4\right]}{B}$$

$$A = W_w \cdot \left[\varepsilon_r \cdot \sigma \cdot \vartheta_{obj}^4 \cdot \tau_a + (1-\varepsilon_r)\sigma \cdot \vartheta_{reflr}^4 \cdot \tau_a + (1-\tau_a)\sigma \cdot \vartheta_a^4 \cdot \tau_a\right]$$

$$B = (1-\varepsilon_r)\sigma \cdot \vartheta_{reflr}^4 \cdot \tau_a^2 + \varepsilon_r \cdot \sigma \cdot \vartheta_{obj}^4 \cdot \tau_a^2 + (1-\tau_a)\sigma \cdot \vartheta_a^4 \cdot \tau_a \tag{16}$$

The air transmittance value can be determined on the bases of formulas presented in [29, 30]. In this case the distance between thermographic camera lens and IR radiator was small. From this reason, it was assumed that the air transmittance value is equal 1.

3. Results and Measurement

At the beginning, uniformity of the distribution of temperature over the surface of the radiator which had been used in the works performed was checked. For this purpose, a thermogram presenting the IR radiator surface which had been painted with the Velvet Coating 811-21 paint was made.

Then the matrix of temperatures on the surface under observation was read out. The difference between the highest and the lowest temperature registered on the surface of the radiator was found to be 1.8 °C.

Then a metal box was put onto the radiator and the rationale for the simplification presented in the formula (12) was verified. For this purpose, the distance between the radiator and the IR window, the distance between the IR window and the thermographic camera lens was measured. In both cases, the distance did not exceed 5 cm. Also, value ϑ_a was measured by means of the GM1365 Data Logger sensor. Values ϑ_a measured during the measurements ranged from 26.9 °C to 27.1 °C. Measurements were taken for all values ϑ_{obj} amounting to 37.9 °C, 40.2 °C, 53.2 °C, 62.3 °C and 72.3 °C.

The value ϑ_{reflr} was measured by placing a bent and straightened aluminium film on the surface of the radiator. IR windows are taken off, too. Then, the thermographic camera presets were changed by selected the value $\varepsilon_r = 1$ and the camera lens – radiator distance = 0 and the thermographic camera indication was read out. It was attempted to take the measurement as fast as possible so as to prevent the aluminium film from being heated up by the IR radiator surface.

The value ϑ_{reflw} was determined in a similar way. In this case, after an IR window has been installed, bent and straightened aluminium film was placed on the IR window surface.

Having determined values ϑ_{reflr} and ϑ_{reflw}, presets of the thermographic camera were made in such a way as to recreate conditions prevailing in the laboratory during the measurements.

For the same preset ϑ_{obj}, the result of a thermographic temperature measurement for an IR radiator not covered by the IR window, the result of a thermographic temperature measurement for a radiator covered with the VFPR-75 window and the result of a thermographic temperature measurement for an IR radiator covered with the FRK100-CL window were read out.

Then, based on equation (16), the transmittance of both IR windows was determined. After determining the transmittance, the measurements were repeated. A computer with Flir Tools software has been added to the measuring system.

The same temperature settings of the IR radiator were chosen. The maximum wavelength of IR radiation emitted by the IR radiator ϑ_m was obtained on the basis of Wien's law. The results of measurements made without the use of infrared windows were used for the calculations.

The settings of thermographic camera were controlled from PC. In the field called "transmittance of the external optical system" the determined value of τ_w has been written. The results obtained during measurement with the VFPR-75 IR window are presented in table 1. The results obtained during measurement with the FRK100-CL IR window are presented in table 2.

4. Conclusions

The result of the undertaken research work is a formula that allows to determine the transmittance of the infrared window. The transmittance of the VFPR-75 and FRK100-CL infrared windows in the temperature range corresponding to the operating temperatures of electrical devices located in the switchgear was also undertaken. The correctness of the determination of the transmittance with the infrared eye was verified experimentally.

Comparing the results of the infrared surface temperature measurements of the IR radiator made without the use of an infrared window with the infrared surface temperature measurements of the radiator in which the infrared window was used and the compensation of the infrared window influence, it can be seen that the greatest temperature difference was about 4 °C (Table 1 and 2). The greatest differences between the measurement results were noticed for the low temperature of

Table 1. The results obtained during thermographic measurement of temperature of IR radiator with VFPR-75 IR window

Tabela 1. Wyniki uzyskane podczas termograficznego pomiaru temperatury promiennika podczerwieni z okienkiem podczerwieni VFPR-75

Lp.	Maximum wavelength of IR radiation λ_m	Calculated value of the transmittance of IR window τ_w	Thermographic measurement of temperature of IR radiator (without IR window)	Thermographic measurement of temperature of IR radiator (with IR window)	Thermographic measurement of temperature of IR radiator (without IR window – the measurement was compensated)
	µm	-	°C	°C	°C
1	9.33	0.52	37.5	31.4	38.9
2	9.25	0.47	40.6	32.5	45.4
3	8.88	0.45	53.4	36.9	54.8
4	8.64	0.37	62.3	40.1	61.9
5	8.39	0.35	72.6	44.6	72.6

Table 2. The results obtained during thermographic measurement of temperature of IR radiator with FRK100-CL IR window

Tabela 2. Wyniki uzyskane podczas termograficznego pomiaru temperatury promiennika podczerwieni z oknem podczerwieni FRK100-CL

Lp.	Maximum wavelength of IR radiation λ_m	Calculated value of the transmittance of IR window τ_w	Thermographic measurement of temperature of IR radiator (without IR window)	Thermographic measurement of temperature of IR radiator (with IR window)	Thermographic measurement of temperature of IR radiator (without IR window – the measurement was compensated)
	µm	–	**°C**	**°C**	**°C**
1	9.33	0.50	36.9	30.9	39.5
2	9.25	0.47	40.4	31.7	45.6
3	8.88	0.40	53.4	36.2	56.7
4	8.64	0.33	62.3	39.1	61.4
5	8.39	0.35	72.6	43.4	70.6

the radiator. For high temperatures of the radiator, the differences between the measurement results decreased. This is a premise that proves the correctness and usefulness of the proposed method.

It should be remembered that the proposed method enables the determination of the approximate values of the transmission window. It can only be used in cases where it is sufficient to use approximate transmittance values for the IR windows. The accuracy with which the transmittance will be determined depends on the precision with which the values of the variables of the equation that allow the transmittance to be determined, will be determined.

References

1. Kuwałek P., *Estimation of Parameters Associated with Individual Sources of Voltage Fluctuations*, "IEEE Transactions On Power Delivery", Vol. 36, No. 1, 2021, 351–361, DOI: 10.1109/TPWRD.2020.2976707.
2. Tian W., Leit C., Jia R., Winter R.M., *Probability Based Circuit Breaker Modeling and Risk Evaluation on Potential Power*, IEEE 7th Annual International Conference on CYBER Technology in Automation, Control, and Intelligent Systems (CYBER), 2017, DOI: 10.1109/CYBER.2017.8446423.
3. Książkiewicz A., Dombek G., Nowak K., *Change in Electric Contact Resistance of Low-Voltage Relays Affected by Fault Current*. "Materials", Vol. 12, No. 13, 2019, 2166-1–2166-11, DOI: 10.3390/ma12132166.
4. Fangrat J., Kaczorek-Chrobak K., Papis B.K., *Fire Behavior of Electrical Installations in Buildings*. "Energies", Vol. 13, No. 23, 2020, DOI: 10.3390/en13236433.
5. Balabozov I., *Experimental Research with Microcontroller System for Defining of Joule Integral of Fuse*, 10th Electrical Engineering Faculty Conference (BulEF), 2018, DOI: 10.1109/BULEF.2018.8646930.
6. Wesołowski M., Chmielak W., *A new sensor system for measuring environmental parameters of switchgear*, Progress in Applied Electrical Engineering (PAEE), 2017, DOI: 10.1109/PAEE.2017.8009024.
7. Zaccara Z., Edelman J.B., Cardone G., *A general procedure for infrared thermography heat transfer measurements in hypersonic wind tunnels*, "International Journal of Heat and Mass Transfer", 2020, DOI: 10.1016/j.ijheatmasstransfer.2020.120419.
8. Altenburg J.S., Straße A., Gumenyuk A., Meierhofer C., *In-situ monitoring of a laser metal deposition (LMD) process: Comparison of MWIR, SWIR and high-speed NIR thermography*. "Quantitative InfraRed Thermography Journal", 2020, DOI: 10.1080/17686733.2020.1829889.
9. Yoon S.T., Park J.C., *An experimental study on the evaluation of temperature uniformity on the surface of a blackbody using infrared cameras*. "Quantitative InfraRed Thermography Journal", 2021, DOI: 10.1080/17686733.2021.1877918.
10. Schuss C., Remes K., Leppänen K., Saarela J., Fabritius T., Eichberger B., Rahkonen T., *Detecting Defects in Photovoltaic Cells and Panels with the Help of Time-Resolved Thermography under Outdoor Environmental Conditions*. [In:] Proceedings of the 2020 IEEE International Instrumentation and Measurement Technology Conference (I2MTC), DOI: 10.1109/I2MTC43012.2020.9128489.
11. Chakraborty B., Billol K.S., *Process-integrated steel ladle monitoring, based on infrared imaging – A robust approach to avoid ladle breakout*. "Quantitative InfraRed Thermography Journal", 2020, 169–191, DOI: 10.1080/17686733.2019.1639112.
12. Tomoyuki T., *Coaxiality Evaluation of Coaxial Imaging System with Concentric Silicon–Glass Hybrid Lens for Thermal and Color Imaging*. "Sensors", Vol. 20, No. 20, 2020, 20, DOI: 10.3390/s20205753.
13. Wollack J.E., Cataldo G., Miller K.H., Quijada A.M., *Infrared properties of high-purity silicon*. "Optics Letters", Vol. 45, No. 17, 2020, 4935–4938, DOI: 10.1364/OL.393847.
14. Singh J., Arora A.S., *Effectiveness of active dynamic and passive thermography in the detection of maxillary sinusitis*, "Quantitative InfraRed Thermography Journal", Vol. 18, No. 4, 2021, 213–225, DOI: 10.1080/17686733.2020.1736456.
15. Holliday T., Kay J.A., *Understanding infrared windows and their effects on infrared readings*, Conference Record of 2013 Annual IEEE Pulp and Paper Industry Technical Conference (PPIC), 2013, 26–33, DOI: 10.1109/PPIC.2013.6656039.
16. Madding R.P., *IR Window Transmittance Temperature Dependence*, [www.exiscan.com/images/files/TechNotes/Madding-IR_window_Transmittance_Temperature_Dependance.pdf].
17. Nguyen T.H., et al, *Enhancing the Quality of the Characteristic Transmittance Curve in the Infrared Region of Range 2.5–7μm of the Optical Magnesium Fluoride (MgF_2) Ceramic Using the Hot-Pressing Technique in a Vacuum Environment*, "Advances in Materials Science and Engineering", 2020, DOI: 10.1155/2020/7258431.
18. Zarei Moghadam R., Ahmadvand H., *Optical and Mechanical Properties of $ZnS/Ge_{0.1}C_{0.9}$ Antireflection Coating on Ge Substrate*. "Iranian Journal of Science and Technology, Transactions A: Science", Vol. 45, 2021, 1491–1497, DOI: 10.1007/s40995-021-01093-5.
19. Kawor E.T., Matteï S., *Emissivity measurements for Nextel Velvet Coating 811-21 between –36 °C and 82 °C*, 15 ECTP Proceedings, DOI: 10.1068/htwu385.
20. PN-HD 60364-5-52:2011 – Instalacje elektryczne niskiego napięcia – Część 5-52: Dobór i montaż wyposażenia elektrycznego – Oprzewodowanie.
21. Chen K., Zhang Y., Wang H., *Effect of acoustic softening on the thermal-mechanical process of ultrasonic welding*, "Ultrasonics", Vol. 75, 2017, 9–21. DOI: 10.1016/j.ultras.2016.11.004.
22. [https://iriss.com/emsd-cast-products/vp-series/vpfc-series] – VPFC Series. Crystal Infrared Windows.
23. [www.fluke.com/en-us/product/thermal-imaging/ir-windows/fluke-100-clkt] – Fluke 100 CLKT IR Window for Outdoor and Indoor Applications.
24. [www.thermokameras.com/Verkauf/Flir%20e-Serie/Datenblatt%20FLIR%20E50%20engl.pdf] – Technical Data FLIR E50.
25. Tran Q.H., Han D., Kang C., Haldar A., Huh J., *Effects of Ambient Temperature and Relative Humidity on Subsurface Defect Detection in Concrete Structures by Active Thermal Imaging*. "Sensors", Vol. 17, No. 8, 2017, DOI: 10.3390/s17081718.
26. Minkina W., *Pomiary termowizyjne – przyrządy i metody*, Wydawnictwo Politechniki Częstochowskiej, Częstochowa 2004.
27. [www.geass.com/wp-content/uploads/filebase/flir/termocamere/e40-e50-e60_comuni/Manuale-termocamere-Flir-E40-E50-E60.pdf] – User's manual FLIR Exx series.
28. Minkina W., Dudzik S., *Infrared Thermography Errors and Uncertainties*; John Wiley & Sons, Ltd.: Chichester, UK, 2009.
29. Minkina W., Klecha D., *Atmospheric transmission coefficient modelling in the infrared for thermovision measurement*, "Journal of Sensors and Sensor System", Vol. 5, 2016, 17–23, DOI: 10.5194/jsss-5-17-2016.
30. Więcek B., de Mey G., *Termowizja w podczerwieni*. Podstawy i zastosowania, Wydawnictwo PAK, Warszawa 2011.

Wyznaczanie transmitancji okien transmisyjnych wykonanych z CaF_2 w zakresie temperatury pracy aparatów elektrycznych

Streszczenie: W artykule przedstawiono streszczenie prac, w wyniku których uzyskano wzór umożliwiający wyznaczenie przybliżonej transmitancji okna transmisyjnego wykorzystywanego w termograficznych pomiarach temperatur urządzeń elektrycznych. Równanie zostało sformułowane po przeanalizowaniu składowych promieniowania podczerwonego docierającego do obiektywu kamery w przypadku, gdy nie zastosowano okna transmisyjnego oraz w przypadku, gdy zastosowano okno transmisyjne. W trakcie wykonywania prac odtworzono warunki panujące podczas termograficznego pomiaru temperatury urządzeń elektrycznych znajdujących się w rozdzielnicy. Przedstawiono system pomiarowy zastosowany w eksperymencie. Omówiono składowe promieniowania podczerwonego docierającego do obiektywu kamery w przypadku, gdy okno transmisyjne było używane oraz w przypadku , gdy okno transmisyjne nie zostało zastosowane. Uzyskane wyniki transmitancji okien VPFR-75 FRK100-CL porównano z danymi pochodzącymi z literatury.

Słowa kluczowe: termografia, urządzenia elektryczne, metrologia

Krzysztof Dziarski, MSc Eng.
krzysztof.dziarski@put.poznan.pl
ORCID: 0000-0002-7877-4116

Assistant at the Institute of Electric Power Engineering, Poznań University of Technology. He attends the fourth year of doctoral studies. In 2017, having completed the second-cycle studies in the same field, he obtained a master's degree in engineering while defending the thesis entitled „Thermographic measurements of micronutrients". He specializes in issues related to temperature measurements, especially thermographic measurements.

Arkadiusz Hulewicz, PhD Eng.
arkadiusz.hulewicz@put.poznan.pl
ORCID: 0000-0001-9342-7430

A graduate of the Faculty of Electrical Engineering at the Poznań University of Technology, where he has been employed since 2001, currently as an assistant in the Department of Metrology of Electronics and Light Technology. Author and co-author of 80 publications. His main scientific interests are metrology, thermovision measurements, bio-measurements and biomedical engineering, optoelectronics, as well as modeling and signal processing.